EUROfusion

WPBB-CPR(18) 21017

A Tassone et al.

MHD mixed convection ow in the WCLL: heat transfer analysis and cooling system optimization

Preprint of Paper to be submitted for publication in Proceeding of 30th Symposium on Fusion Technology (SOFT)

This work has been carried out within the framework of the EUROfusion Consortium and has received funding from the Euratom research and training programme 2014-2018 under grant agreement No 633053. The views and opinions expressed herein do not necessarily reflect those of the European Commission.

MHD mixed convection flow in the WCLL: heat transfer analysis and cooling system optimization

Alessandro Tassone[1]*, Gianfranco Caruso[1], Fabio Giannetti[1], Alessandro Del Nevo[2]

[1] *DIAEE Nuclear Section - Sapienza University of Rome, Corso Vittorio Emanuele II, 244, 00186, Roma, Italy*

[2] *ENEA FSN-ING-PAN, ENEA CR Brasimone, 40032, Camugnano (BO), Italy*

Abstract

In the Water-Cooled Lithium Lead (WCLL) blanket, a critical problem faced by the design is to ensure that the breeding zone (BZ) is properly cooled by the refrigeration system to keep the structural materials under the maximum allowed temperature by the design criteria. CFD simulations are performed using ANSYS CFX to assess the cooling system performances accounting for the magnetic field effect in the sub-channel closest to the first wall (FW). Here, intense buoyancy forces ($Gr \approx 10^{10}$) interact with the pressure-driven flow ($Re \approx 10^3$) in a MHD mixed convection regime. A constant magnetic field, parallel to the toroidal direction, is assumed with intensity $B = 4.4\,T$. The walls bounding the channel and the water pipes are modeled as perfectly conducting. The magnetic field is found to dampen the velocity fluctuations triggered by the buoyancy forces and the flow is similar to a forced convection regime. The PbLi heat transfer coefficient is reduced to one-third of its ordinary hydrodynamic value and, consequently, hot-spots between the nested pipes and at the FW are observed, where $T_{Max} \approx 1000\,K$ Optimization strategies for the BZ cooling system layout are proposed and implemented in the CFD model, thus fulfilling the design criterion.

Keywords: Magnetohydrodynamics (MHD), blanket engineering, WCLL, mixed convection, CFD

1. Introduction

The Water Cooled Lithium-Lead (WCLL) blanket is under development as a candidate for implementation in the DEMOnstration fusion reactor [1]. In the WCLL, Lithium Lead (PbLi) is employed as breeder, pressurized water at 155 MPa as first wall (FW) and breding zone (BZ) coolant, and Eurofer steel as structural material. A single module segmentation approach is employed with the blanket being segmented only in the toroidal direction [2]. To preserve the Eurofer mechanical properties, the PbLi temperature must not exceed 823 K (550 °C) during normal operation [3]. Four alternative configurations are currently being studied to identify advantages and key issues to select the reference configuration that will be further developed in the next years.

The magnetohydrodynamic (MHD) effect on the performances is a key design issues for liquid metal blankets. Transition to the MHD regime is accompanied by severe increase in pressure drop, flow stabilization and heat transfer degradation [4]. To limit the pressure drop, the WCLL minimizes the PbLi velocity and employs a non-electrically conductive fluid as coolant. Due to this strategy, the intense temperature gradient fostered by the neutronic power deposition generates buoyancy forces that add to the main forced convection flow, thus generating in the BZ a MHD mixed convection regime. Previous thermal-hydraulic studies have reported that buoyancy forces are fundamental in shaping the temperature distribution in the WCLL [5]. The rationale for this study is to evaluate the BZ cooling system performances when the magnetic field is applied and the role played by the buoyancy forces.

2. Problem formulation

For this study, the configuration v2017.T02 of the WCLL outboard blanket is considered [6]. The BZ is occupied by long rectangular channels that run all along the blanket poloidal height with the breeder flowing upward inside them. The blanket cross-section assumes the appearance of a checkerboard composed by $4\,x\,8$ channels. To ensure the BZ refrigeration, double-walled pipes are inserted horizontally from the back part of the segment through openings drilled in the toroidal-poloidal stiffening plates. Two nested U-pipes constitute the elementary component of the BZ cooling system (BZCS), which is responsible for the refrigeration of a 4-channel radial stack spanning from FW to the back supporting structure. This cooling element is then repeated uniformly for the channel poloidal extension. Therefore, the pitch (p_v) between cooling elements is a characterizing parameter for the blanket

*Corresponding author:
Email address: alessandro.tassone@uniroma1.it (Alessandro Tassone[1])

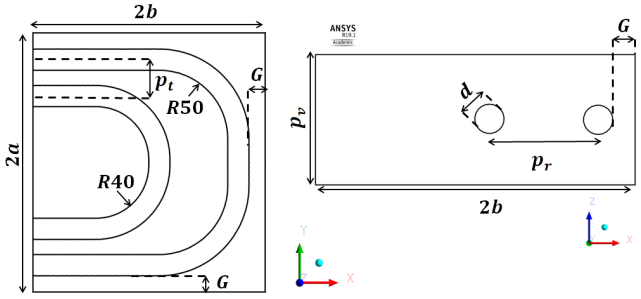

Fig. 1. Cell geometry: radial-toroidal (left), radial-poloidal (right)

Table 1
Geometry parameters, length in mm [6]

Toroidal half-length	a	82	Vertical pitch	p_v	60
Radial half-length	b	73.5	Radial pitch	p_r	50
Pipe ext. diameter	d_o	13.5	Toroidal pitch	p_t	23
Pipe int. diameter	d_i	8	Pipe-wall distance	G	10.25

layout. An overview of the problem geometry is available in Figure 1, whereas the main geometrical parameters are collected in Table 1.

The governing equations for a steady, induction-less, incompressible and laminar MHD flow are obtained by the combination of the Navier-Stokes and Maxwell sets. Choosing the electric potential formulation and modeling the buoyancy forces with the Boussinesq approximation [7], they can be written as following

$$\nabla \cdot \vec{v} = 0 \tag{1}$$

$$(\vec{v} \cdot \nabla)\vec{v} = -\frac{1}{\rho}\nabla p + \nu\nabla^2\vec{v} + \frac{1}{\rho}\vec{j} \times \vec{B} - \beta\Delta T\vec{g} \tag{2}$$

$$\rho c_p(\vec{v} \cdot \nabla)T = k\nabla^2 T + Q \tag{3}$$

$$\vec{j} = \sigma(-\nabla\phi + \vec{v} \times \vec{B}) \tag{4}$$

$$\nabla \cdot \vec{j} = 0 \tag{5}$$

Combining the Ohm's law (4) and charge conservation (5), it is found the Poisson equation

$$\nabla^2\phi = \nabla \cdot (\vec{v} \times \vec{B}) \tag{6}$$

which, once solved, provides the electric potential ϕ distribution and, through (4), the current density $\vec{j}$. The symbols Q and $\vec{B}$ represent, respectively, the volumetric rate of internal power generation and the applied magnetic field. In (3), the source term due to the joule heating is neglected. In a ordinary hydrodynamic (OHD) mixed convection flow, the main parameters of interest are the Reynolds (Re), Grashof (Gr) and Prandtl (Pr) numbers and the interaction parameter Gr/Re^2. If $Gr/Re^2 \gg 1$, the flow is dominated by the buoyancy forces , vice versa for $Gr/Re^2 \ll 1$. For a MHD flow, we must add the Hartmann number $M = Ba(\sigma/\rho\nu)^{0.5}$, ratio of electromagnetic and viscous forces, and Lykoudis number $Ly = M^2/Gr^{0.5}$, ratio of electromagnetic and buoyancy forces. [7]. Finally, the wall conductance ratio $c_w = \sigma_w t_w/\sigma L$ represents the effect of the electrical boundary conditions on the flow features, i.e. insulating walls lead to an higher resistance for the current paths and, therefore, to lower Lorentz forces compared with electro-conductive walls [7].

Table 2
Material physical properties, in brackets the temperature assumed for constant

PbLi (T_{ref}) [8]		
Density [kg/m^3]	ρ	9675.21
Expansion coefficent [K^{-1}]	β	$1.23{\cdot}10^{-4}$
Specific heat [J/kgK]	c_p	188.49
Permeability [H/m]	μ_0	$4\pi \cdot 10^{-7}$
Kinematic viscosity [m^2/s]	ν	$\frac{1.87{\cdot}10^{-4}}{\rho} e^{(1400/T)}$
Thermal conductivity [W/mK]	κ	$1.95 + 1.95 \cdot 10^{-2}\,T$
Electrical conductivity [S/m]	σ	$(1.02 \cdot 10^{-4} + 4.26 \cdot 10^{-8}\,T)^{-1}$
Eurofer (T_{ext}) [9], Water (T_{ext}) [10]		

3. Numerical model

Due to the temperature range foreseen in the model, i.e. $T = 600 \div 825\,K$, the temperature dependence is preserved for the PbLi physical properties varying $\Delta\Phi(T_{Max}, T_{Min}) > \pm 5\%$ with respect to the value at $T_{ref} = 710\,K$ (see Table 2 for a detailed implementation overview). The average Prandtl number for the PbLi is $Pr = 0.011$.

The no-slip boundary condition (BC) is enforced at the pipe and duct surfaces. Periodic BCs are imposed at the bottom (inlet) and top (outlet) surfaces of the model with an absolute mass flow rate $\Gamma = 0.431$ kg/s^{-1}, equivalent to a mean velocity $u_0 = 1.825$ mm/s^{-1}[2].

Duct walls are adiabatic. A source term is employed to represent the power deposition in the PbLi using the function $Q = (6.5844) \cdot e^{8.8605x}$ MW/m^3, where $x = [-0.0735, 0.0735]$ is the radial coordinate, as described by Martelli et al.[5]. The Heat Transfer Coefficient (HTC) BC is employed to model the heat transfer water-side without simulating the coolant and accounting for the pipe thermal resistance. This method reduces the problem to a single computational domain, containing the PbLi. The external HTC is calculated as $h_{ext} = (1/h_{pipe} + 1/h_{H2O})^{-1} = 1.05 \cdot 10^4$ Wm^{-2}K^{-1}, where $h_{pipe} = 2\kappa_{EU}/(d_i ln(d_o/d_i))$ and h_{H2O} is calculated from the Dittus-Boelter correlation assuming an average velocity $u_{H2O} = 5$ ms^{-1}. Water and Eurofer properties are evaluated at the average water temperature $T_{ext} = 584.65\,K$ [2].

A uniform and constant magnetic field is applied in the toroidal (y) direction $B = 4.4$ T [11]. The solid surfaces are considered as perfectly conducting ($c_w = \infty$). This assumption simplifies the model by removing the need to simulate the solid walls and is conservative in terms of the Lorentz force experienced by the flow [7].

An unstructured grid is employed with prismatic inflation layer at the duct and pipe surfaces to resolve the boundary layers. The layer thickness is $\delta = O(M^{-1})$ thus,

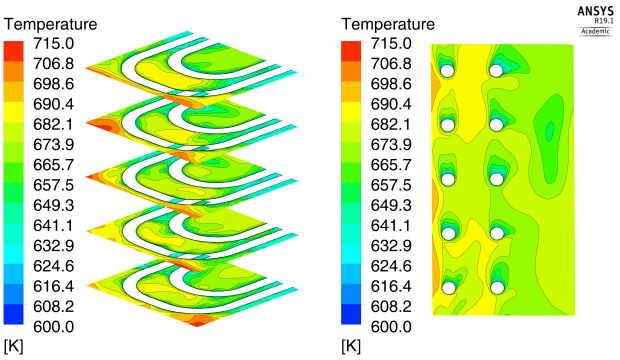

Fig. 2. OHD 5-cell stack temperature distribution on the horizontal planes passing through the pipe center (left) and the vertical central plane (right)

for high magnetic fields and poorly conducting walls, the layer scale is comparable to the viscous sublayer for turbulent flows and the layer is "active": it provides a path for the current closure, thus defining the flow features. Assuming a perfectly conducting wall allows to treat the layer as "passive", since it does not carry any current, and to relax the mesh resolution to 2 nodes in the layer thickness, enough to follow the velocity gradient therein.

The MHD model of ANSYS CFX has been validated in the past up to $M = 10^4$ for pressure-driven and buoyancy-driven benchmarks for a range of wall conductance ratio $c_w = [0, \infty]$. Further details about the validation process are reported in [11].

4. Results and discussion

First an OHD simulation is performed employing a geometry featuring five cooling elements. In absence of magnetic field, the channel is strongly dominated by buoyancy forces ($Gr = 10^{10}, Re = 1400$) and, since $Gr/Re^2 \gg 1$, the forced convection contribution is negligible. In fact, the flow becomes turbulent and it is simulated employing the Shear Stress Transport (SST) model. The velocity scale observed is $v \approx 15$ cm s^{-1}, almost two orders of magnitude higher than the one due to forced convection, and vortices of length scale equal to p_v appear between the cooling elements. Due to these phenomena, the heat transfer is extremely efficient and the maximum temperature is well below the threshold ($T_{Max,OHD} = 714\,K$). In Figure 2, it can be seen how hotspots are present in the FW corners.

When the magnetic field is applied, the flow becomes dominated by Lorentz forces and, due to the high field intensity ($M = 8500, Ly \gg 1$), is laminar and steady with a velocity scale comparable to the only forced convection. The vortices observed in OHD are completely suppressed, although the buoyancy forces still shape the velocity profile with characteristic features like opposing jets close to the FW and cooling pipes [7]. The heat transfer is dampened and becomes dominated by the conduction mechanism. Considering the heat flux removed from the pipe surface

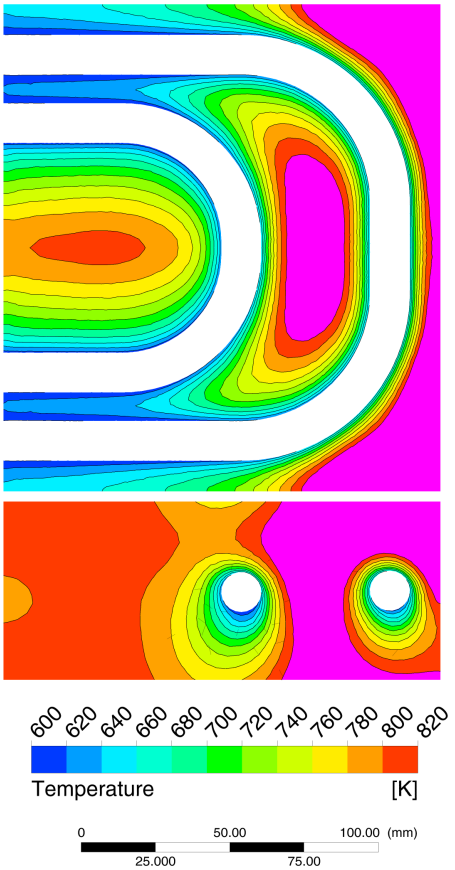

Fig. 3. MHD cell temperature distribution on the horizontal plane passing through the pipe center (top) and the vertical central plane (bottom)

(q''), the heat transfer coefficient (h_{LM}) between PbLi and pipe surface is defined as $h_{LM} = \left(\frac{\bar{T}-T_{ext}}{q''} - \frac{1}{h_{ext}}\right)^{-1}$, with ($\bar{T}$) the average PbLi temperature calculated on the horizontal plane across the pipe center. It is found that $h_{LM} \approx 3500$ Wm^{-2}K^{-1} for the MHD case, one-third of the value calculated in OHD. The maximum temperature recorded in the cell is 1031 K. In Figure 3, the temperature contour is plotted considering $T = 820$ K as the scale ceiling. Hotspots are present at the corners and in the radial gap between the pipes.

4.1. BZCS optimization

Previous thermo-hydraulic studies have suggested that the FW cooling system passively refrigerate the nearby BZ region removing among 5%÷10% of the total power deposited with a mean heat flux q_{FW} = -130 kW/m^2 [5]. This phenomenon is represented in the CFD model assuming a constant heat flux removed from the FW. The maximum temperature trend with q_{FW} is shown in Table 3. Corner hotspots are efficiently cooled by this strategy, but only for the highest flux considered the temperature falls below the threshold.

Successively, the vertical pitch (p_v) is reduced, thus decreasing the amount of power to be removed by the single

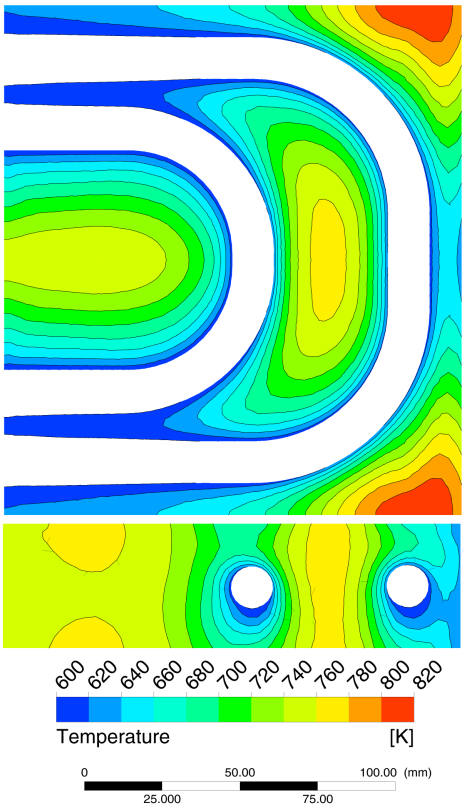

Fig. 4. MHD cell optimized temperature distribution on the horizontal plane passing through the pipe center (top) and the vertical central plane (bottom)

Table 3
Maximum temperature in the cell versus optimization parameter. For p_v reduction, q_{FW} = -100 kW/m^2 is assumed

Passive FW cooling		Vertical pitch reduction	
qFW [kW/m^2]	Tmax [K]	p_v [mm]	Tmax [K]
0	1031	60	898
-50	941	55	873
-100	885	50	854
-150	844	45	835
-200	817	40	823

cooling element. FW passive refrigeration is assumed at q_{FW} = -100 kW/m^2. Maximum temperature trend is available in Table 3. For p_v = 40 mm, the temperature in the cell is everywhere below the criterion but, as it is possible to observe in Fig. 4, corner hotspots are still present. It should be noted that in absence of FW refrigeration, even for the lowest p_v considered the maximum temperature exceeds 900 K.

5. Conclusions

A CFD model of the FW channel of the configuration v2017.T02 of the WCLL blanket is realized to assess the BZCS performances in MHD operative conditions. The magnetic field suppresses buoyancy-induced velocity oscillations reverting the intense turbulent OHD flow into laminar state. The PbLi-side heat transfer coefficient is reduced to one-third, with conduction becoming the dominant mechanism, and the temperature reaches above 1000 K. The design criterion $T_{max} \leq 823\,K$ is met by introducing a moderate amount of passive refrigeration from the FW (q_{FW} = -100 kW/m^2) and reducing the distance between cooling elements to p_v = 40 mm.

Further optimization is possible by modifying the pipe layout, e.g. bringing them closer to the walls, and considering realistic walls. For the latter, increased peak velocities are foreseen close to the cooling pipe according to the asymptotic theory developed by Buhler, which would enhance the heat transfer [7]. However, reliance on the FW cooling system to provide BZ refrigeration is all but a sound design strategy and should be avoided. Manufacturing issues in the realization of the U-pipe layout is another drawback that must be considered in the selection of the reference design for the WCLL blanket[12].

Acknowledgements

This work has been carried out within the framework of the EUROfusion Consortium and has received funding from the Euratom research and training programme 2014-2018 under grant agreement No 633053. The views and opinions expressed herein do not necessarily reflect those of the European Commission.

References

[1] F. Cismondi, et al., Progress in eu breeding blanket design and integration, Fusion Engineering and Design (2018).
[2] A. Tassone, et al., Recent progress in the wcll breeding blanket design for the demo fusion reactor, IEEE Transactions on Plasma Science 46 (2018) 1446–1457.
[3] J. Aubert, et al., Optimization of the first wall for the demo water cooled lithium lead blanket, Fusion Engineering and Design 98 (2015) 1206–1210.
[4] S. Smolentsev, et al., MHD thermofluid issues of liquid-metal blankets: phenomena and advances, Fusion Engineering and Design 85 (2010) 1196–1205.
[5] E. Martelli, et al., Thermo-hydraulic analysis of eu demo wcll breeding blanket, Fusion Engineering and Design 130 (2018) 48–55.
[6] R. Mozzillo, et al., Assessment on DEMO water cooled lithium lead alternative design configuration, (this conference) (2018).
[7] U. Müller, L. Bühler, Magnetofluiddynamics in channels and containers, Springer Science & Business Media, 2013.
[8] U. Jauch, et al., Thermophysical properties in the system Li-Pb, KIT, 1986.
[9] K. Mergia, N. Boukos, Structural, thermal, electrical and magnetic properties of Eurofer 97 steel, Journal of Nuclear Materials 373 (2008) 1–8.
[10] W. Wagner, H.-J. Kretzschmar, IAPWS industrial formulation 1997 for the thermodynamic properties of water and steam, IAPWS-IF97 (2008) 7–150.
[11] A. Tassone, et al., CFD simulation of the magnetohydrodynamic flow inside the WCLL breeding blanket module, Fusion Engineering and Design 124 (2017) 705–709.
[12] D. Sornin, A. Li Puma, C. Schweier, WPBB-DEL- BB-7.1.1-T003-D001, EFDA D 2NBQ6U, Assessment of Manufacturing Technologies for Blanket Development (WCLL) / 2017 status of WCLL manufacturing activities, Eurofusion, 2018.